FAST VARIATIONAL LEVEL SET BASED IMAGE SEGMENTATION VIA TWO-SCALE FILTERING MODEL

Lingfeng Wang, Ying Wang and Chunhong Pan

NLPR, Institute of Automation, CAS, {lfwang,ywang,chpan}@nlpr.ia.ac.cn

ABSTRACT

One major difficulty in medical image segmentation is intensity inhomogeneity, which manifests itself with a slow intensity variation over the whole image domain. Recently, a local binary fitting (LBF) model has been proposed to solve this problem within level set segmentation framework. However, the LBF model has two main problems, i.e., high computational cost and sensitivity to initialization. By analyzing the LBF model, we find that the most computational part is the calculation of two cluster images, which need to be updated in each iteration during the evolution of level set function. With this observation in mind, we propose a novel two-scale filtering (TSF) model, in which the two cluster images can be pre-calculated before evolution. Additionally, we implicitly utilize order constraint to restrict the order of two cluster images. As a result, the proposed TSF model is less sensitive to initialization. Extensive experiments on real medical images illustrate the desirable performances, as compared with the state-of-the-art models.

***Index Terms*—** Image segmentation, level set, active contour, region-based, two-scale filtering model

1. INTRODUCTION

Segmentation plays an important role in medical image computing, and it has a wide range of applications. Over the past decades, many segmentation methods have been proposed. Among them, level set segmentation methods, especially the region-based level set methods, attract more attention for their special advantages over the other methods, i.e., sub-pixel segmentation accuracy and arbitrary topological transformation.

To the best of our knowledge, the first region-based segmentation method is proposed in [1], called the Chan and Vese (CV) model. In this method, two values are adopted to fit the pixel intensities in the internal and external of the segmented regions. Due to the utilization of pixel intensity statistical information, the CV model is less sensitive to initialization and noise. Especially, the segmented contour of this model may not stop at weak edges. It is worth noting that the CV model and its variations, such as the total variation CV (TVCV) model in [2, 3] and the model proposed in [4], are called global region-based methods. However, the CV model always fails to segment the interested object out when the input image presents intensity inhomogeneity, which manifests itself with a slow intensity variation in the same tissue over the whole image domain.

To address intensity inhomogeneity problem, many local region-based methods have been proposed. One of the most famous local region-based method is proposed in [5], called the local binary fitting (LBF) model. The core idea behind the LBF model is to consider the CV model locally by introducing a Gaussian kernel function. Compared with the CV model, the LBF model usually provides more accurate segmentation results, especially when the input images are inhomogeneous. However, the LBF model has two major limitations, which are the superiorities of CV model. First, it is sensitive to the initialization, especially when the size of local Gaussian kernel is small. Second, the computational cost of the LBF model is large, due to the utilization of convolution operation. Recently, many models have been presented by proposing new local region-based models or improving the LBF model.

Motivated by the LBF model, local Gaussian fitting (LGF) model is proposed in [6]. Compared with binary distribution in the LBF model, Gaussian distribution in the LGF model is more accurate in the representation of the distribution of local pixel intensities. The local linear classification (LLC) model is introduced in [7]. The LLC model is less sensitive to initialization. Unfortunately, both the LGF and LLC models need more computational cost than the LBF model. The local image fitting (LIF) model proposed in [8] is faster than the LBF model, however, it is still sensitive to initialization. Moreover, it has a lower segmentation accuracy than the LBF model. The local CV model is proposed in [9] by incorporating local image information. It is less sensitive to initialization compared with LBF. The local signed difference model is proposed in [10]. The main superiority of this model is its speed (similar with the global methods). However, the segmentation results are not satisfied.

To solve the initialization problem, a number of improved model derived from the LBF model are proposed. For example, a new model that combines the CV and LBF models through a weighting strategy is proposed in [11]. However, choosing an appropriate weighting value is a hard problem, since the degree of intensity inhomogeneity is unknown. In [12], the local order model is added to the original LBF model to ensure that the local binary fitting values hold global consistent order. However, the order model is hard to be extended from the two-phase model to the multi-phase case. Same with the order model, [13] proposes a contrast constraint. The order constraint can be regarded as a special contrast constraint with the contrast value being zero. Motivated by [3], the convex LBF model, which is independent to initialization, is proposed in [14]. The above models are less sensitive to initialization, compared with the LBF model. However, their computational cost is still very high.

In this paper, we propose a new two-scale filtering (TSF) model to decrease the computational cost as well as reduce initialization sensitivity of the LBF model. Firstly, in the object scale, a Bilateral filtering operation is utilized to obtain the local clusters, named as object image. Then, in the context scale, a Gaussian filtering operation is adopted to obtain the mixed result of local clusters, named as context image. By calculating the difference of context and object images, the complementary local clusters, named complementary image, is obtained. Finally, order operation is utilized to separate local foreground and background clusters.

This work is supported by the National Natural Science Foundation of China (Grant No. 61773377 and 91646207).

2. BRIEF REVIEW ON LBF AND MOTIVATION

The LBF model [5] tries to find a contour, which is represented by a level set function ϕ, to divide the whole image domain Ω into two non-overlapped parts. And it segments the object from background by minimizing the following energy function:

$$\begin{aligned} &E_{\text{LBF}}(\phi, C_1, C_2) \\ &= \lambda_1 \iint K_\sigma(\mathbf{x}-\mathbf{y})|I(\mathbf{y})-C_1(\mathbf{x})|^2 H_\epsilon(\phi(\mathbf{y}))\mathrm{d}\mathbf{y}\mathrm{d}\mathbf{x} \qquad (1) \\ &+ \lambda_2 \iint K_\sigma(\mathbf{x}-\mathbf{y})|I(\mathbf{y})-C_2(\mathbf{x})|^2 (1-H_\epsilon(\phi(\mathbf{y})))\mathrm{d}\mathbf{y}\mathrm{d}\mathbf{x}, \end{aligned}$$

where $H_\epsilon(x) = \frac{1}{2}\left[\frac{1}{2} + \frac{2}{\pi}\arctan\left(\frac{x}{\epsilon}\right)\right]$ is a smooth version of the Heaviside function. The standard gradient descent is used to minimize the energy function of Eqn. (1), given by

$$\frac{\partial \phi}{\partial t} = -\delta_\epsilon(\phi)(\lambda_1 e_1 - \lambda_2 e_2),$$

where t is the time step, $\delta_\epsilon(x) = \frac{1}{\pi}\frac{\epsilon}{\epsilon^2+x^2}$ is the derivation of $H_\epsilon(x)$, and the terms e_1 and e_2 are defined as

$$e_i(\mathbf{x}) = \int_{y\in\Omega} K_\sigma(\mathbf{y}-\mathbf{x})|I(\mathbf{x})-C_i(\mathbf{y})|^2 \mathrm{d}y, \quad i=1,2 \qquad (2)$$

yielding

$$C_1 = \frac{K_\sigma \otimes [H_\epsilon(\phi) I]}{K_\sigma \otimes H_\epsilon(\phi)}, \quad C_2 = \frac{K_\sigma \otimes [(1-H_\epsilon(\phi))I]}{K_\sigma \otimes (1-H_\epsilon(\phi))}, \qquad (3)$$

where $\otimes$ is the convolution operation, and the two values C_1 and C_2 can be regarded as two cluster images.

The core behind the LBF model is the calculation of the two cluster images C_1 and C_2. In the LBF model, they are updated during the evolution of the level set function. From Eqn. (3), the calculation of the two cluster images is very time consuming due to the utilization of the convolution operation. Accordingly, to reduce the amount of calculation, it is very necessary to pre-calculate the two cluster images, which is the main issue addressed in this paper.

3. THE PROPOSED METHOD

3.1. Two-scale Filtering Model

After performing image segmentation, the segmentation contour (or the zero level of the level set function) is desired to match the boundary of the object. Combining with Eqn. (3), when desirable segmentation result is obtained, $C_1(\mathbf{x})$ and $C_2(\mathbf{x})$ will be the mean values of the intensities of local foreground and background respectively. In other words, to obtain $C_1(\mathbf{x})$ (or $C_2(\mathbf{x})$), we can collect the pixels that belong to foreground (or background), and then calculate the mean value. This process is very close to the idea of the Bilateral filtering. Hence, in the object scale, the local cluster is obtained by Bilateral filtering of the input image:

$$B = \text{BF}(I; p), \qquad (4)$$

where BF(.) is the Bilateral filtering operator, and p represents the parameters for the Bilateral filtering operation. In our method, the Guided filtering in [15] is selected as the Bilateral filtering.

The Bilateral filtered image B mixes foreground and background clusters together. Specifically, for each pixel $B(\mathbf{x})$ in the Bilateral filtered image B, we cannot distinguish it from foreground to background, that is, it may be the foreground cluster $C_1(\mathbf{x})$ or the background cluster $C_2(\mathbf{x})$. Moreover, the Bilateral filtered image B only tells us one cluster for each pixel. In other words, for each pixel located at $\mathbf{x}$, if it belongs to foreground, the Bilateral filtered result $B(\mathbf{x})$ can only provide the foreground cluster, i.e., $C_1(\mathbf{x}) = B(\mathbf{x})$, but cannot provide the corresponding background cluster $C_2(\mathbf{x})$. It is similar for the pixels located at background. To solve above problems, we propose a context scale filter, in which each pixel is a combination of foreground and background clusters, given by

$$G = \text{GF}(I; q), \qquad (5)$$

where GF(.) is the Gaussian filtering operator with parameter q. For each pixel $G(\mathbf{x})$ in the Gaussian filtered image G, it mixes foreground and background clusters together, thus,

$$G(\mathbf{x}) = \alpha(\mathbf{x})C_1(\mathbf{x}) + (1-\alpha(\mathbf{x}))C_2(\mathbf{x}), \quad \forall \mathbf{x} \in \Omega, \qquad (6)$$

where $0 \le \alpha(\mathbf{x}) \le 1$ is a mixture factor. Here, we assume $\alpha(\mathbf{x}) = 0.5$, which indicates the mixture is equal. Thereby, the mixture function is simplified as

$$2G(\mathbf{x}) = C_1(\mathbf{x}) + C_2(\mathbf{x}), \quad \forall \mathbf{x} \in \Omega. \qquad (7)$$

We define a new complementary image $\bar{B}$ of the object image B,

$$\bar{B} = 2G - B, \qquad (8)$$

where B and G are the object and context filtered results.

The complementary image $\bar{B}$ holds the similar property of the object image B. In other words, it also mixes foreground and background clusters. Fortunately, the two images are just complementary with each other. Thus, by applying order constraint proposed in [12] on the object image B and the complementary image $\bar{B}$, the foreground and background images C_1 and C_2 are estimated by

$$\begin{aligned} C_1(\mathbf{x}) &= \max(B(\mathbf{x}), \bar{B}(\mathbf{x})), \\ C_2(\mathbf{x}) &= \min(B(\mathbf{x}), \bar{B}(\mathbf{x})), \quad \forall \mathbf{x} \in \Omega, \end{aligned} \qquad (9)$$

where $\max(\cdot)$ and $\min(\cdot)$ are maximum and minimum functions.

3.2. Level-set Formulation of Segmentation Model

Based on the calculated foreground and background images C_1 and C_2 in Eqn. (9), the objective function of our two-scale filtering (TSF) model under the level set formulation is

$$\begin{aligned} E_{\text{TSF}}(\phi) = \lambda_1 &\int_{\mathbf{x}\in\Omega} |I(\mathbf{x}) - C_1(\mathbf{x})|^2 H_\epsilon(\phi(\mathbf{x}))\mathrm{d}\mathbf{x} \\ + \lambda_2 &\int_{\mathbf{x}\in\Omega} |I(\mathbf{x}) - C_2(\mathbf{x})|^2 (1-H_\epsilon(\phi(\mathbf{x})))\mathrm{d}\mathbf{x}. \end{aligned} \qquad (10)$$

In the TSF model, the foreground and background pixels are desired to be close to the foreground and background clusters, respectively. By incorporating the length and signed distance function regularization terms, the final energy function is

$$F(\phi) = E_{\text{TSF}}(\phi) + \nu L(\phi) + \mu P(\phi), \qquad (11)$$

where ν and μ are two weighting constants. The second term

$$L(\phi) = \int_{\mathbf{x}\in\Omega} |\nabla H_\epsilon(\phi(\mathbf{x}))| \, \mathrm{d}\mathbf{x}$$

is the contour length term, which constricts the length of the segmentation contour, and the third term

$$P(\phi) = \int_{\mathbf{x}\in\Omega} \frac{1}{2}\left(|\nabla\phi(\mathbf{x})| - 1\right)^2 \mathrm{d}\mathbf{x}$$

is the regularization term proposed in [16], which characterizes the deviation of the level set function from a signed distance function.

Table 1. Comparison of the data terms of CV, LBF and TSF models.

Model	Data Term	Complexity	Fitting
CV	$-\delta_\epsilon(\phi)\,(\lambda_1 d_1 - \lambda_2 d_2)$ $d_i(\mathbf{x}) = \lvert I(\mathbf{x}) - c_i\rvert^2,\ i = 1, 2.$	$\mathcal{O}(h \times w \times t)$	Global
LBF	$-\delta_\epsilon(\phi)(\lambda_1 e_1 - \lambda_2 e_2)$ $e_i(\mathbf{x}) = \int_{\mathbf{y}\in\Omega} K_\sigma(\mathbf{y}-\mathbf{x})\lvert I(\mathbf{x}) - C_i(\mathbf{y})\rvert^2 \mathrm{d}\mathbf{y},\ i = 1, 2$	$\mathcal{O}(h \times w \times k^2 \times t)$	Local
TSF	$-\delta_\epsilon(\phi)\,(\lambda_1 f_1 - \lambda_2 f_2)$ $f_i(\mathbf{x}) = \lvert I(\mathbf{x}) - C_i(\mathbf{x})\rvert^2,\ i = 1, 2.$	$\mathcal{O}(h \times w \times t)$	Local

3.3. Optimization and Implementation

The standard gradient descent method is adopted to minimize the objective energy function. Specifically, we utilize the steepest descent method to minimize the energy function $F(\phi)$ in Eqn. (11) with respect to the level set function ϕ. The gradient flow equation is given by

$$\begin{aligned}\frac{\partial \phi}{\partial t} &= -\frac{\partial F(\phi)}{\partial \phi} \\ &= -\delta_\epsilon(\phi)\,(\lambda_1 f_1 - \lambda_2 f_2) \\ &\quad +\nu\delta_\epsilon(\phi)\mathrm{div}\left(\frac{\nabla\phi}{|\nabla\phi|}\right) + \mu\left(\nabla^2\phi - \mathrm{div}\left(\frac{\nabla\phi}{|\nabla\phi|}\right)\right) \end{aligned} \tag{12}$$

where

$$f_i(\mathbf{x}) = |I(\mathbf{x}) - C_i(\mathbf{x})|^2,\ i = 1, 2. \tag{13}$$

The first term $-\delta_\epsilon(\phi)\,(\lambda_1 f_1 - \lambda_2 f_2)$ derived from the TSF model is named as the data term.

To implement our method, the level set function ϕ is first initialized as a binary function as follows:

$$\phi^0(\mathbf{x}) = \begin{cases} \rho, & \mathbf{x} \in \Omega_0 - \partial\Omega_0 \\ 0, & \mathbf{x} \in \partial\Omega_0 \\ -\rho, & \mathbf{x} \in \Omega - \Omega_0 \end{cases} \tag{14}$$

where Ω_0 is a subset of the image domain Ω, and $\partial\Omega_0$ is the boundary of Ω. Then, the level set function ϕ is evolved according to

$$\begin{aligned}\frac{\phi^{t+1} - \phi^t}{\Delta t} &= -\delta_\epsilon(\phi^t)\,(\lambda_1 f_1 - \lambda_2 f_2) \\ &\quad +\nu\delta_\epsilon(\phi^t)\mathrm{div}\left(\frac{\nabla\phi^t}{|\nabla\phi^t|}\right) + \mu\left(\nabla^2\phi^t - \mathrm{div}\left(\frac{\nabla\phi^t}{|\nabla\phi^t|}\right)\right) \end{aligned} \tag{15}$$

which is the discrete version of Eqn. (12).

3.4. Advantages over the State-of-the-art Models

In this subsection, we describe the main advantages of the proposed TSF model over the classical CV and LBF models by comparing their data terms, which are used to guide the evolution of level set functions. The data terms of CV, LBF and TSF models are listed in Table 1, from which we can see that the differences arise from the calculation of d_i, e_i and f_i. In the following, we compare them in computational complexity and image fitting.

Computational Complexity: We only focus on the computational complexity analysis for the evolution of level set function, because it is the most time-consuming part in level set based segmentation. The contour length term $\delta_\epsilon(\phi^t)\mathrm{div}(\frac{\nabla\phi^t}{|\nabla\phi^t|})$ and the regularization term $(\nabla^2\phi^t - \mathrm{div}(\frac{\nabla\phi^t}{|\nabla\phi^t|}))$ are independent to the data term, and the computational complexity of them are proportional to the size of image and the number of iterations, which is $\mathcal{O}(h \times w \times t)$, where h and w are height and width of the input image, respectively, and t is the number of iterations. In CV, the computational complexity of the data term is also $\mathcal{O}(h \times w \times t)$. Hence, the computational complexity of CV is $\mathcal{O}(h \times w \times t)$. In LBF, convolutions are performed to obtained e_i, thereby, its computational complexity is $\mathcal{O}(h \times w \times k^2 \times t)$, where k is the size of Gaussian kernel. The two smooth functions C_1 and C_2 are updated in each iteration. As illustrated in Eqn. (3), the computational complexity is also $\mathcal{O}(h \times w \times k^2 \times t)$ due to the utilization of convolution. Hence, the computational complexity of LBF is $\mathcal{O}(h \times w \times k^2 \times t)$. In TSF, the data term can be calculated in advanced due to C_1 and C_2 can be pre-computed, which indicates that the computational cost of data term is zero. Combining with the contour length and regularization terms, the computational complexity of TSF is $\mathcal{O}(h \times w \times t)$.

Image Fitting: In CV, the global two values c_1 and c_2 are utilized to fit all foreground and background pixels. As a result, when the input image is inhomogeneous, CV fails to segment out the object (or foreground). Both LBF and TSF adopt local values $C_1(\mathbf{x})$ and $C_2(\mathbf{x})$ to fit the local foreground and background pixels. Hence, both of them can solve the intensity inhomogeneous problem.

To sum up, the TSF model has the same computational complexity with the *global* CV model, while it can use local image information to solve intensity inhomogeneity as the *local* LBF model.

4. EXPERIMENTAL RESULTS

In this section, we compare our model with the state-of-the-art approaches, including CV [1], SBGFR [4], LIF [8], LBF [5], LL-C [7] and CK [17] in following aspects, i.e., segmentation accuracy and run speed. Eight medical images acquired via different techniques, MRI, X-ray, and ultrasound are selected for both qualitative and quantitative evaluations. For the quantitative comparison, **IoU** $= \frac{\mathcal{M}_{\text{seg}} \cap \mathcal{M}_{\text{truth}}}{\mathcal{M}_{\text{seg}} \cup \mathcal{M}_{\text{truth}}}$ (Intersection over Union) is utilized as the evaluation criterion, where $\mathcal{M}_{\text{seg}}$ and $\mathcal{M}_{\text{truth}}$ are segmented and ground truth foreground masks, respectively. The ground truths are created by manual segmentation.

4.1. Comparison

The comparisons on eight medical images are shown in Fig. 1. The main difficulties of these images are listed as follows:

1. Intensity inhomogeneity in MRI may be caused by many factors, such as radio-frequency non-uniformity, static field inhomogeneity and patient-specific interactions.

2. The difficulties of vessel image arise from three aspects. First, the vessel structure is slightness. Segmenting slightness objects is a well-known difficult problem. Second, the contrast between vessel

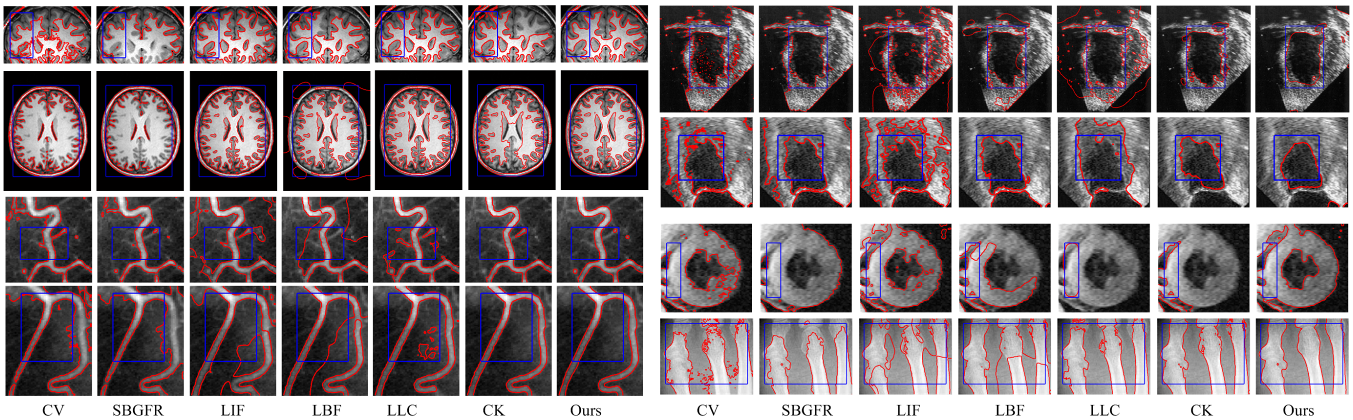

Fig. 1. Comparative results of the proposed method with CV, SBGFR, LIF, LBF, LLC and CK on two MRI brain images. The initial and final contours are marked in blue and red, respectively.

Table 2. Comparison of **RoU**s on the images from Fig. 1. The best and second results are indicated by **bold face** and underline.

	CV	SBGFR	LIF	LBF	LLC	CK	Ours
(1)	0.414	0.554	0.542	0.567	**0.864**	0.640	0.790
(2)	0.545	0.491	0.610	0.580	**0.791**	0.673	0.688
(3)	0.635	0.674	0.499	0.189	0.728	**0.962**	0.814
(4)	0.535	0.479	0.283	0.245	0.831	**0.995**	0.893
(5)	0.202	0.207	0.287	0.583	0.209	0.746	**0.747**
(6)	0.380	0.387	0.266	0.545	0.338	0.685	**0.802**
(7)	0.224	0.150	0.205	0.143	0.118	0.115	**0.225**
(8)	0.727	0.664	0.401	0.577	0.837	**0.960**	0.957
Mean	0.458	0.451	0.386	0.429	0.589	0.722	**0.740**

and background is so low that in some area it is even hard for human nature to distinguish it from its local background. Third, the intensity inhomogeneity also exists in these two images.

3. There is almost no intensity inhomogeneity in heart image and two ultrasound images. Unfortunately, the noise, such as block and spot noise, is very large in these images.

4. In X-ray bone image, intensity inhomogeneity is also very serious. In some parts, such as in the bone joints, the contrast between bone and non-bone background is also very low.

As shown in Fig. 1, only the proposed LSF model can successfully segment out all objects. For the global region-based methods, i.e., CV and SBGFR, the details cannot be segmented out. With arbitrary initialization, the segmentation contours of CK stick on the smooth regions. For LIF and LBF, the segmentation results mix the object and background together. The quantitative comparison of the above eight images with **IoU** evaluation criterion are illustrated in Table 2. As shown in this table, our method achieves top two ranks in eight images and the mean result is best.

4.2. Run Speed

The run speeds on the eight medical images are also evaluated. The comparative results are shown in Table 3. The run speed is proportional to the iteration number. For all the methods, we use convergence of level set evolution as the termination criteria. From Table 3, we can see that our method has the comparative speed to two global methods, i.e., CV and SBGFR on most data. Specifically, our method is slower in two ultrasound images. The main reason is that in these two images, our model needs large iteration numbers. It is worth noting that LLC is slower than the other methods. The main reason is that the time step in this method is very small. Thereby, it needs a large number of iterations to achieve convergence.

Table 3. Run speed (in second) of the eight images in Fig. 1.

	CV	SBGFR	LIF	LBF	LLC	CK	Ours
(1)	0.181	0.198	5.63	9.91	22.6	20.0	0.239
(2)	0.434	0.501	11.7	10.2	98.8	62.2	0.406
(3)	0.179	0.208	11.4	5.38	23.1	5.23	0.254
(4)	0.202	0.216	15.3	5.5	35.0	4.77	0.281
(5)	0.480	0.529	13.3	14.5	108	11.4	2.68
(6)	0.154	0.168	4.75	2.70	21.1	7.33	1.00
(7)	0.225	0.262	7.32	7.15	1.31	4.57	0.233
(8)	0.252	0.303	8.83	25.9	98.7	78.1	0.557
Mean	0.192	0.217	7.11	7.39	37.2	17.6	0.514

5. CONCLUSION AND DISCUSSION

In this paper, a new TSF model is proposed to solve image segmentation problem. Compared with the state-of-the-art approaches, our model has the following two superiorities. First, our method has higher segmentation accuracy than the other local region based methods. Second, our method is very fast. Experimental results illustrate that our method has the similar speed as the global region-based methods, such as the traditional CV model.

However, our method also has some limitations, which will be the effort direction of future work. First, when the initialization is very well, the other local region-based methods, such as LLC and CK, may have higher segmentation accuracies than our model. The main reason is that the local cluster images are fixed in the evolution of level set function (or pre-calculated before evolution). Although the run speed can be accelerated, the local cluster images cannot benefit from the updating of level set function. As a result, the small scale tissue structure may not be well segmented out in our model. To improve the TSF model, in the future, we will try hard to find new models, in which the local cluster images can be close to those of other local models. Second, due to implicit utilization of order constraint, our model cannot segment bright and dark objects simultaneously. One potential solution is to introduce multi-phase technique, which will be a future direction.

6. REFERENCES

[1] Tony F. Chan and Luminita A. Vese, "Active contours without edges," *IEEE Transactions on Image Processing*, vol. 10, pp. 266–277, 2001.

[2] Mila Nikolova, Selim Esedoglu, and Tony F. Chan, "Algorithms for finding global minimizers of image segmentation and denoising models," *SIAM Journal of Applied Mathematics*, vol. 66, no. 5, pp. 1632–1648, 2006.

[3] Tom Goldstein, Xavier Bresson, and Stanley Osher, "Geometric applications of the split bregman method: Segmentation and surface reconstruction," *Journal of Scientific Computing*, vol. 45, no. 1-3, pp. 272–293, 2010.

[4] Kaihua Zhang, Lei Zhang, Huihui Song, and Wengang Zhou, "Active contours with selective local or global segmentation: A new formulation and level set method," *Image and Vision Computing*, vol. 28, no. 4, pp. 668–676, 2010.

[5] Chunming Li, Chiu-Yen Kao, John C. Gore, and Zhaohua Ding, "Minimization of region-scalable fitting energy for image segmentation," *IEEE Transactions on Image Processing*, vol. 17, no. 10, pp. 1940–1949, 2008.

[6] Li Wang, Jim Macione, Quansen Sun, Deshen Xia, , and Chunming Li, "Level set segmentation based on local gaussian distribution fitting," in *Asian Conference on Computer Vision*, 2009, pp. 293–302.

[7] Ying Wang, Shiming Xiang, Chunhong Pan, LingFeng Wang, and Gaofeng Meng, "Level set evolution with locally linear classification for image segmentation," *Pattern Recognition*, vol. 46, no. 6, pp. 1734–1746, 2013.

[8] Kaihua Zhang, Huihui Song, and Lei Zhang, "Active contours driven by local image fitting energy," *Pattern Recognition*, vol. 43, no. 4, pp. 1199–1206, 2010.

[9] Xiaofeng Wang, De-Shuang Huang, and Huan Xu, "An efficient local chan-vese model for image segmentation," *Pattern Recognition*, vol. 43, no. 3, pp. 603–618, 2010.

[10] LingFeng Wang, Huai-Yu Wu, and Chunhong Pan, "Region-based image segmentation with local signed difference energy," *Pattern Recognition Letters*, vol. 34, no. 6, pp. 637–645, 2013.

[11] Li Wang, Chunming Li, Quansen Sun, Deshen Xia, and Chiu-Yen Kao, "Active contours driven by local and global intensity fitting energy with application to brain MR image segmentation," *Computerized Medical Imaging and Graphics*, vol. 33, no. 7, pp. 520–531, October 2009.

[12] LingFeng Wang, Zeyun Yu, and Chunhong Pan, "A unified level set framework utilizing parameter priors for medical image segmentation," *Science China Information Sciences*, vol. 55, pp. 1–14, 2012.

[13] Xiaojing Bai, Chunming Li, Quan-Sen Sun, and De-Shen Xia, "Contrast constrained local binary fitting for image segmentation," in *Advances in Visual Computing, 5th International Symposium, ISVC 2009, Las Vegas, NV, USA, November 30 - December 2, 2009, Proceedings, Part I*, 2009, pp. 886–895.

[14] Hongda Mao, Huafeng Liu, and Pengcheng Shi, "A convex neighbor-constrained active contour model for image segmentation," in *Proceedings of the International Conference on Image Processing, ICIP 2010, September 26-29, Hong Kong, China*, 2010, pp. 793–796.

[15] Kaiming He, Jian Sun, and Xiaoou Tang, "Guided image filtering," *IEEE Trans. Pattern Anal. Mach. Intell.*, vol. 35, no. 6, pp. 1397–1409, 2013.

[16] Chunming Li, Chenyang Xu, Changfeng Gui, and Martin D. Fox, "Level set evolution without re-initialization: A new variational formulation," in *IEEE Conference on Computer Vision and Pattern Recognition*, 2005, pp. 430–436.

[17] LingFeng Wang and Chunhong Pan, "Robust level set image segmentation via a local correntropy-based k-means clustering," *Pattern Recognition*, vol. 47, no. 5, pp. 1917–1925, 2014.